Inhibition of MDM2 attenuates neointimal hyperplasia via suppression of vascular proliferation and inflammation

Hashimoto, Toru
Department of Cardiovascular Medicine, Kyushu University, Graduate School of Medical Sciences

Ichiki, Toshihiro
Department of Advanced Therapeutics for Cardiovascular Diseases, Kyushu University Graduate School of Medical Sciences | Department of Cardiovascular Medicine, Kyushu University, Graduate School of Medical Sciences

Ikeda, Jiro
Department of Cardiovascular Medicine, Kyushu University, Graduate School of Medical Sciences

Narabayashi, Eriko
Department of Cardiovascular Medicine, Kyushu University, Graduate School of Medical Sciences

他

出版情報：Cardiovascular Research. 91 (4), pp.711-719, 2011-04-14. Oxford University Press
バージョン：

Inhibition of MDM2 Attenuates Neointimal Hyperplasia via Suppression of Vascular Proliferation and Inflammation

Toru Hashimoto[1], Toshihiro Ichiki[1, 2], Jiro Ikeda[1], Eriko Narabayashi[1], Hirohide Matsuura[1], Ryohei Miyazaki[1], Keita Inanaga, Kotaro Takeda[1, 2], Kenji Sunagawa[1]

Departments of Cardiovascular Medicine[1], and Advanced Therapeutics for Cardiovascular Diseases[2], Kyushu University Graduate School of Medical Sciences, Fukuoka, Japan

Short title: MDM2 Inhibition Attenuates Neointimal Hyperplasia

Correspondence to Toshihiro Ichiki, MD, PhD, Department of Cardiovascular Medicine, Kyushu University Graduate School of Medical Sciences, 3-1-1 Maidashi, Higashi-ku, 812-8582 Fukuoka, Japan.

E-mail: ichiki@cardiol.med.kyushu-u.ac.jp

TEL: +81-92-642-5358, FAX: +81-92-642-5374

Total words: 5619, Figures: 5, Supplementary data (Supplementary Figures: 3)

Abstract

Aims: Tumor protein p53 plays an important role in vascular remodeling process as well as oncogenesis. p53 is negatively regulated by murine double minute 2 (MDM2). A recently developed MDM2 inhibitor, nutlin-3, is a nongenotoxic activator of the p53 pathway. So far, the effect of MDM2 inhibition on vascular remodeling has not been elucidated. We therefore investigated the effect of nutlin-3 on neointima formation.

Methods and Results: Nutlin-3 up-regulated p53 and its downstream p21 in VSMCs. DNA synthesis assay and flow cytometric analysis revealed that nutlin-3 inhibited platelet-derived growth factor (PDGF)-induced vascular smooth muscle cell (VSMC) proliferation by cell cycle arrest. This inhibitory effect was abrogated in p53-siRNA-transfected VSMCs. Furthermore, nutlin-3 inhibited PDGF-stimulated VSMC migration. Treatment with nutlin-3 attenuated neointimal hyperplasia at 28 days after vascular injury in mice, associated with up-regulation of p53 and p21. BrdU incorporation was decreased at 14 days after injury in nutlin-3-treated mice. TUNEL assay showed that nutlin-3 did not exaggerate apoptosis of the injured vessels. Infiltration of macrophages and T lymphocytes, and mRNA expression of chemokine (C-C motif) ligand-5, interleukin-6, and intercellular adhesion molecule-1 was decreased in the injured vessels of nutlin-3-administered mice. Nutlin-3 suppressed

NF-κB activation in VSMCs, but not in p53-siRNA transfected VSMCs.

Conclusions: MDM2 antagonist nutlin-3 inhibits VSMC proliferation, migration, and NF-κB activation, and also attenuates neointimal hyperplasia after vascular injury in mice, associated with suppression of vascular cell proliferation and inflammatory response. Targeting MDM2 might be a potential therapeutic strategy for the treatment of vascular proliferative diseases.

Key Words: MDM2, p53, proliferation, inflammation, neointima

Introduction

Vascular proliferation and inflammation, in which vascular smooth muscle cells (VSMCs) are involved profoundly, contribute to the pathophysiology of cardiovascular diseases including atherosclerosis, post-intervention restenosis, vein bypass graft failure, and transplant vasculpoathy. Although the drug-eluting stent (DES) technology has reduced restenosis after coronary intervention, further elucidation of molecular mechanisms of vascular inflammation and proliferation is required for the retainment of vascular patency and reduction of cardiovascular events.[1-3]

The tumor protein p53 (Tp53) governs fundamental cellular processes such as apoptosis, cell cycle arrest, senescence, DNA repair, and cellular metabolism by regulating the transcription of many genes in response to stress signals.[4] p53 is believed to be involved in cardiovascular pathogenesis, however, the role of p53 in atherosclerotic diseases is Janus-faced. p53 deficiency exacerbates atherosclerosis in genetic dyslipidemic mice models,[5-8] while p53 overexpression enhances atherosclerotic plaque rupture.[9]

p53 expression is regulated by numerous proteins; more than 160 studies have been reported to date. Among them, murine double minute 2 (MDM2) is regarded outstanding because they function as specific and indispensable inhibitors

of p53 during embryonic development and their expression level is frequently affected in cancers.[10] MDM2 inhibits p53 transcriptional activity by occluding the transactivation domain to interrupt a recruitment of co-activators, and ubiquitinates the C-terminal domain promoting degradation by proteasome.[11]

MDM2 is overexpressed in human atherosclerotic tissues,[12] and in VSMCs of patients with primary aldosteronism,[13] indicating that MDM2 participates in pathological vascular remodeling. These studies also suggest that p53 might be suppressed by MDM2 in vascular proliferating process; therefore reactivation of the p53 pathway may be a novel therapeutic strategy for the treatment of vascular remodeling.

Disruption of the MDM2-p53 interaction has attracted an interest as a novel therapeutic strategy for cancers. Recently, a small molecule inhibitor of MDM2-p53 binding, nutlin-3, was developed.[14] Nutlin-3 has antitumor effects by p53 activation in various cancer cells,[15] and *in vivo* administration induces tumor regression in mice.[14, 16-19]

These studies prompted us to investigate the effects of nutlin-3 on vascular remodeling process including VSMC proliferation and gene expression. In the present study, we showed that nutlin-3 inhibited platelet-derived growth factor

(PDGF)-induced VSMC proliferation and NF-κB activation, and also attenuated neointimal hyperplasia after arterial injury in mice.

Materials and Methods

Materials

Dulbecco's modified Eagle's medium (DMEM) was purchased from Invitrogen (Carlsbad, CA, USA). Fetal bovine serum (FBS) was purchased from Nichirei Biosciences (Tokyo, Japan). Recombinant rat PDGF-BB was purchased from R&D Systems (Minneapolis, MN, USA). Bovine serum albumin (BSA), bromodeoxyuridine (BrdU), propidium iodide (PI), anti-α-tubulin antibody, and FITC-conjugated anti-α-smooth muscle actin antibody were from Sigma-Aldrich (St. Lois, MO, USA). Nutlin-3 was purchased from Cayman Chemical (Ann Arbor, MI, USA). Antibodies against p38MAPK, phospho-p38MAPK, ERK1/2, phospho-ERK1/2, JNK/SAPK, phospho-JNK/SAPK, p53, and histone H3 were purchased from Cell Signaling Technology (Beverly, MA, USA). Antibodies against p53, MDM2, PECAM-1, and Mac-3 were from Santa Cruz Biotechnology (Santa Cruz, CA, USA). Anti-p21 antibodies were from BD Biosciences Pharmingen (San Diego, CA, USA) and Imgenex (San Diego, CA, USA). Anti-CD3 antibody was from Abcam (Cambridge, MA, USA).

Cell Cultures

VSMCs were isolated from the thoracic aorta of Sprague-Dawley rats (Kyudo Co., Saga, Japan). Cells were maintained in DMEM supplemented with 10% FBS at 37℃ in a humidified atmosphere in 5% CO_2 in air. Before stimulation, cells were serum-starved in DMEM with 0.1% BSA for 2 days.

Measurement of DNA Synthesis

VSMCs pretreated with nutlin-3 (10 μmol/L) were stimulated with PDGF-BB (50 ng/mL) for 24 hours and pulsed with [^{3}H]-thymidine (1 μCi/mL) for the last 6 hours. Following washing with PBS, cells were incubated with 10% trichloroacetic acid, rinsed with a mixture of ethanol and diethylether (2:1), and dissolved in 0.5N NaOH. The incorporation of [^{3}H]-thymidine into cells was measured by a liquid scintillation counter.

Flow cytometry

For cell cycle analysis, harvested VSMC were washed in PBS, and fixed in cold 70% ethanol. After treatment with RNase A (25 mg/mL) at 37℃ for 60 minutes, cells were stained with PI (50 μg/mL) at 4℃ for 30 minutes. Samples were analyzed by BD FACSCalibur (Becton, Dickinson & Co., Franklin Lakes, NJ, USA). The cell cycle distribution was analyzed by ModFit LT software (Verity Software House, Topsham, ME, USA). Apoptosis analysis was performed by using Annexin V-FITC Apoptosis Detection Kit I (BD Biosciences Pharmingen) and BD FACSCalibur according to the

manufacturer's instructions.

Small-interfering RNA (siRNA) transfection

p53-targeting siRNA (#M-080060-00, a mixture of 4 siRNA: 5' GAGAAUAUUUCACCCUUAA 3'; 5' GCGACAGGGUCACCUAAUU 3'; 5' GUACUCAAUUUCCCUCAAU 3'; 5' CCACUAUCCACUACAAGUA 3') and negative control non-targeting siRNA (D-001210-03) were purchased from Thermo Scientific Dharmacon (Lafayette, CO, USA). siRNA was introduced into VSMCs by a lipid transfection method. siRNA was mixed with lipofectamine RNAiMAX (Invitrogen, Carlsbad, CA, USA) in Opti-MEM I Reduced Serum Medium (Invitrogen) and incubated for 20 minutes at room temperature. VSMCs were transfected with the siRNA-lipofectamine complexes and incubated for 48 hours at 37℃ in a CO_2 incubator, and then used in the experiments.

Real-time Reverse Transcription Polymerase Chain Reaction (RT-PCR)

Total RNA was extracted by the acid guanidinium thiocyanate-phenol chloroform extraction method. RNA was reverse-transcribed using ReverTra Ace qPCR RT kit (TOYOBO, Osaka, Japan) according to the manufacturer's instructions. Real-time quantitative PCR (qPCR) was performed using THUNDERBIRD SYBR qPCR Mix (TOYOBO) and the Applied Biosystems 7500 Real Time PCR System (Applied Biosystems, Foster City, CA, USA). Relative expression levels were determined by

comparative Ct (ΔΔCt) method. *Hprt1* mRNA was used for standardization. Primer sequences used for amplification are as follows: <rat> *Tp53* (forward) 5’ GAGGTCGGCTCCGACTATACCA 3’, (reverse) 5’ AAAGCTGTCCCGTCCCAGAAG 3’; *Hprt1* (forward) 5’ TCCTCATGGACTGATTATGGACA 3’, (reverse) 5’ TAATCCAGCAGGTCAGCAAAGA 3’; <mouse> *Ccl5* (forward) 5' ACCAGCAGCAAGTGCTCCAA 3', (reverse) 5' TGGCTAGGACTAGAGCAAGCAATG 3'; *Il6* (forward) 5’ CCACTTCACAAGTCGGAGGCTTA 3’, (reverse) 5’ GCAAGTGCATCATCGTTGTTCATAC 3’; *Icam1* (forward) 5’ GGCACCCAGCAGAAGTTGTT 3’, (reverse) 5’ CCTCAGTCACCTCTACCAAG 3’; *Hprt1* (forward) 5’ TTGTTGTTGGATATGCCCTTGACTA 3’, (reverse) 5’ AGGCAGATGGCCACAGGACTA 3’

Western blot Analysis

Cells were harvested with lysis buffer composed of 1×RIPA, 1% aprotinin, 10 μmol/L pepstatin A, 1 mmol/L PMSF, and 2.5 μg/mL leupepsin. Equal amounts of protein samples were subjected to SDS-PAGE, and transferred to a polyvinylidene difluoride membrane (Immobilon-P, Millipore Corp., Billerica, MA, USA). After blocking with 5% skim milk, the membrane was incubated with a primary antibody, followed by a horseradish peroxidase (HRP)-conjugated secondary antibody. Blots were detected by chemiluminescence system using ECL Western Blotting Detection Reagent (GE

Healthcare UK). The membrane was exposed to X-ray film. The protein expression level was quantified by densitometry.

Cell Migration Assay (*in vitro* scratch assay)

VSMCs were plated onto the 35-mm dish coated with type I collagen and grown to be confluent. Following pretreatment with nutlin-3 (10 μmol/L) for 24 hours, the VSMC monolayer was scraped with a pipet tip to create scratch wound, and then stimulated with PDGF-BB (50 ng/mL). After 24-hour incubation, the number of cells which migrated into the scratch area was counted under microscopy.

DNA-binding ELISA for NF-κB

TransAM NF-κB p65 assay Kit (Active Motif, Carlsbad, CA, USA) was used. Equal amounts of nuclear extracts were added to the 96-well plate containing NF-κB consensus sequence and subjected to binding reaction for 1 hour. Following incubation with anti-NF-κB p65 antibody for 1 hour, samples were incubated with HRP-conjugated anti-IgG antibody for 1 hour. Then samples were subjected to colorimetric reaction and absorbance at 450 nm was read by Mithras LB940 (Berthold Technologies, Bad Wildbad, Germany).

Animal Experiments

All procedures were approved by the institutional animal use and care committee, and conducted in accordance with institutional guidelines and Guide for the Care

and Use of Laboratory Animals (NIH Publication No. 85-23, revised 1996). C57B/6J male mice were purchased from CLEA Japan (Tokyo, Japan) and fed a normal chow. Mice (10-week-old) were anesthetized by intraperitoneal injection of 50 mg/kg pentobarbital, and then arterial wire injury was performed by insertion of a wire (0.38mm in diameter. #C-SF-15-15, COOK, Bloomington, IN, USA) into the femoral artery as described previously.[20] Mini-osmotic pumps (Alzet, DURECT, Cupertino, CA, USA) delivering nutlin-3 (5 mg/kg/day) were placed into the intraperitonal space immediately after the vascular injury operation. BrdU (25 mg/kg) was injected at 24 hours and 1 hour prior to tissue harvest. Mice were euthanized with injection of overdose pentobarbital. Harvested femoral arteries were fixed in 10% neutral-buffered formaldehyde solution. For RNA isolation, tissues were snap-frozen in liquid nitrogen.

Morphometric Analysis and Immunohistochemistry

Neointimal and medial areas were quantified by NIH ImageJ software. Percent stenosis was determined as the ratio of the intimal area and the area inside the internal elastic lamina × 100. For enzyme immunohistochemistry, paraffin-embedded tissue sections were deparaffinized and rehydrated, and then autoclaved in 10 mmol/L citrate buffer for antigen retrieval. Following quenching endogenous peroxidase and blocking with 3% skim milk, sections were incubated

with primary antibodies at 4℃ overnight. After incubation with biotinylated secondary antibodies and treatment with streptoavidine-horseradish peroxidase conjugate, sections were incubated in 3,3'-diaminobenzidine (DAB) solution and counterstained with hematoxylin. For fluorescent immunohistochemistry, sections were incubated with FITC-conjugated primary antibodies for 2 hours at room temperature, and then observed by fluorescent microscopy. Apoptotic cells were detected by the terminal deoxynucleotidyl transferase dUTP nick end labeling (TUNEL) method with Apoptosis in situ Detection Kit (Wako Pure Chemical Industries, Osaka, Japan). Incorporated BrdU was detected using Cell Proliferation Kit (GE Healthcare UK).

Statistical Analysis

Experimental data were analyzed by one-way ANOVA and Fisher's *post hoc* test. Results are expressed as mean±SEM. Values of $p<0.05$ were considered statistically significant.

Results

Nutlin-3 activates p53 pathway and inhibits cellular proliferation and migration in VSMCs

At first, the effect of nutlin-3 on rat VSMC proliferation was examined. DNA synthesis

assay showed that enhanced [^{3}H]-thymidine uptake induced by PDGF was dose-dependently suppressed by nutlin-3 treatment in VSMCs (Figure 1A). We further assessed the effects of nutlin-3 on VSMC migration by *in vitro* scratch assay. Treatment with nutlin-3 attenuated VSMC migration induced by PDGF (Figure 1B).

We next verified whether nutlin-3 induces p53 in VSMCs. p53 protein expression was up-regulated by treatment with nutlin-3 (Figure 1C). p21 and MDM2, p53 downstream target molecules, were also up-regulated by nutlin-3 (Figure 1C), indicating functional activation of the p53 pathway in VSMCs. MAP kinases are known to be important mediators of PDGF signaling pathway.[21] However, nutlin-3 had no effects on the phosphorylation of p38MAPK, ERK1/2, and JNK/SAPK stimulated by PDGF (Supplementary Figure I). In order to exclude the possibility that the reduction of the number of proliferating cells was caused by apoptosis, we also evaluated VSMC apoptosis by flow cytometry. Treatment with nutlin-3 did not instigate apoptosis at basal condition, and did not enhance H_2O_2-induced apoptosis either (Figure 1D). These results imply that the inhibitory effect of nutlin-3 on VSMC proliferation may not be attributable to inhibition of MAP kinases or induction of apoptosis.

Nutlin-3 induces cell cycle arrest in a p53-dependent manner in VSMCs

The effect of nutlin-3 on the cell cycle profile in rat VSMCs was analyzed by flow

cytometry. To confirm whether the inhibitory effect of nutlin-3 on cell proliferation depends on p53, assays were performed with or without p53 knock down by siRNA. Transfection of p53-targeting siRNA significantly down-regulated p53 mRNA expression in VSMCs, while transfection of control siRNA did not affect p53 mRNA expression levels (Figure 2A). Flow cytometric analysis revealed that the increase in the proportion of S-phase and the decrease in the proportion of G1-phase induced by PDGF was attenuated by treatment with nutlin-3 in VSMCs transfected with control siRNA (Figure 2B), whereas nutlin-3 failed to prevent cell cycle progression stimulated by PDGF in VSMCs transfected with p53-siRNA (Figure 2B). The cell cycle arrest-inducing effect of nutlin-3 was also abrogated in p53-deficient mouse VSMCs (Supplementary Figure II). These results suggest that nutlin-3 inhibited VSMC proliferation via p53-dependent cell cycle arrest at G1 phase.

Nutlin-3 attenuates neointimal hyperplasia after vascular injury

We next explored the effects of nutlin-3 on neointimal formation in mice. Administration of nutlin-3 (5 mg/kg/day) had no apparent effects on body weight and hemodynamics including blood pressure and heart rate (data not shown). No sickness behavior and mortality occurred during the experimental period. No apparent macroscopic organ damage and tissue abnormalities were observed in nutlin-3-administered mice. Neointimal hyperplasia provoked by arterial wire-injury

was significantly attenuated in nutlin-3-treated mice compared with control mice at 28 days after injury (Figure 3A and 3B). In both groups, most of the neointimal tissues were composed of α-smooth muscle actin (α-SMA) positive VSMCs (Figure 3C). Sirius Red staining revealed that the neointimal tissues in both groups were also abundant in collagen fibers (Figure 3D). The collagen fiber hues under observation by polarizing microscopy were yellowish similarly in each group, suggesting that there would not be differences in collagen fiber properties affecting tissue stability (Figure 3D). Immunostaining of PECAM-1 showed that the luminal surface of the neointima was overlaid with endothelial cells in both control and nutlin-3 groups, indicating that administration of nutlin-3 did not impair re-endothelialization (Figure 3E). These results suggest that treatment with nutlin-3 attenuates neointimal overgrowth without affecting vascular tissue integrity. Expression of p53 and p21 was up-regulated in the vascular tissues of nutlin-3-administered mice compared with untreated mice (Figure 3F). MDM2 expression was unaffected by treatment with nutlin-3 (Figure 3F).

Effects of MDM2 inhibition on vascular proliferation and inflammation

Incorporation of BrdU into the neointima cells was decreased in nutlin-3-treated mice compared with control mice at 14 days but not 28 days after vascular injury (Figure 4A). There were only a few TUNEL-positive apoptotic cells detected at 7 days after injury, however, enhanced apoptosis was not observed in nutlin-3-administered mice

(Figure 4B). TUNEL-positive cells were not detected either in control or nutlin-3 groups at 14 and 28 days after injury (Figure 4B). These results suggest minor contribution of apoptosis to the inhibition of neointimal growth by nutlin-3. Vascular inflammation is mainly regulated by NF-κB-dependent gene transcription,[22] and involved in the progression of vascular proliferative diseases.[1-3] Since it has been reported that p53 inhibits NF-κB pathway,[23-27] we also investigated whether nutlin-3 affects NF-κB-regulated gene expression and infiltration of inflammatory cells in injured vascular tissues. Infiltration of macrophages and T lymphocytes in the injured vessels was significantly attenuated in nutlin-3-administered mice (Figure 4C and 4D). RT-qPCR of the injured vessels showed that mRNA expression of NF-κB-regulated genes including chemokine (C-C motif) ligand 5 (CCL5), interleukin-6 (IL-6), and intercellular adhesion molecule-1 (ICAM-1) was suppressed in nutlin-3-treated mice (Figure 5A).

Nutlin-3 suppresses nuclear activation of NF-κB dependently on p53

To elucidate the mechanism of the decrease in proinflammatory gene expression in the injured vessels of nutlin-3-treated mice, we performed NF-κB DNA-binding ELISA using cultured rat VSMCs. Treatment with nutlin-3 significantly attenuated NF-κB activation induced by TNFα in VSMCs transfected with control siRNA (Figure 5B), while this inhibitory effect was abrogated in VSMCs transfected with p53-targeting

siRNA (Figure 5B). The NF-κB-suppressing effect of nutlin-3 was also abolished in p53-deficient mouse VSMCs (Supplementary Figure III). These results suggest that the inhibitory effect of nutlin-3 on NF-κB activation depends on p53.

Discussion

In the present study, we demonstrated that an MDM2 inhibitor nutlin-3 suppressed VSMC proliferation through cell cycle arrest at G1 phase. The effects of nutlin-3 depend on p53 because nutlin-3 failed to show any effects on VSMCs transfected with p53-targeting siRNA and p53-deficient VSMCs. We also demonstrated that treatment with nutlin-3 attenuated neointimal hyperplasia after vascular injury without increasing vascular tissue vulnerability. Inhibition of vascular cell proliferation, inflammatory cell infiltration, and proinflammatory gene expression was observed in the injured vessels of nutlin-3-administered mice, suggesting that nutlin-3 ameliorated maladaptive vascular remodeling through inhibition of neointimal VSMC growth and modulation of inflammatory process. Infiltration of leukocytes mediated by chemokines and VSMC proliferation are critical to neointimal growth after vascular injury.[3] Therefore, a therapeutic strategy against both cell proliferation and vascular inflammation is rational for efficacious remedy for neointimal hyperplasia. MDM2 inhibitors may have unique therapeutic potential

because it is capable of inhibiting NF-κB activation in as well as inducing cell cycle arrest via p53 activation.

Previous reports have demonstrated that the protective role of p53 against neointimal hyperplasia.[28-34] Such an effect has been thought to be brought about by increased apoptosis or inhibition of proliferation of VSMCs. These studies adopted, however, p53 gene transfer by adenovirus vectors, liposome, or transgenic technique, which are technically and ethically difficult to utilize in the clinical settings. Indeed p53 activation can be instigated by anticancer drugs, which is inevitably associated with DNA damage leading to enhanced apoptosis and tissue damage.[15] The fact that nutlin-3 can activate p53 by inhibition of MDM2, not by DNA damage-triggered induction, encourages us to apply the “p53 activation” to the conquest of vascular proliferative diseases practically.

Since MDM2 is a downstream target gene of p53 as well as p21, MDM2 up-regulation by treatment with MDM2 inhibitor nutlin-3 is thought to result from a negative feedback mechanism. Although the kinetics of p53, p21, and MDM2 in VSMCs seems parallel in time in our results, up-regulation of p21 and MDM2 may follow the induction of p53 in a delayed fashion at the early phase after stimulation with nutlin-3 like seen in other cells.[18, 19]

Nutlin-3 inhibits cell proliferation by p53 activation leading to p21-mediated

cell cycle arrest at G1 phase. p53 can also induce apoptosis in response to stress signals, but apoptosis-inducing effect of p53 might depend on cell type or require further cofactors or modifications.[35] Nutlin-3 does not induce apoptosis of vascular endothelial cells,[36] neutrophils, and macrophages.[23] In this study, acceleration of apoptosis was not observed either in nutlin-3-treated VSMCs or neointima of nutlin-3-administered mice after vascular injury, which is consistent with previous studies. Very early apoptosis after vascular injury is relevant for vascular remodeling. SMC apoptosis is induced immediately after vascular injury, attaining to the peak in 0.5-1 hour, and declines rapidly.[37] Considering the fact that administration of nutlin-3 was instituted by implantation of mini-osmotic pumps following vascular injury and the concentration of nutlin-3 would reach steady state for at least several hours, it is unlikely that nutlin-3 affects apoptosis which occurs very early after vascular injury in our models.

p53 activation is known to suppress NF-κB-dependent gene expression.[23-25] It has been reported that p53 and NF-κB can repress the transactivation of each other via competition for transcriptional co-activator p300/CREB-binding protein (CBP).[26, 27] We showed that nutlin-3 suppressed NF-κB activation in VSMCs. Though a direct proof of NF-κB activation is lacking in our animal experiments, inhibition of the expression of NF-κB-regulated proinflammatory genes such as CCL5, IL-6, and

ICAM-1 suggests that nutlin-3 may suppress NF-κB activation in injured vessels as shown in cultured VSMCs. These observations about the effects of MDM2 inhibitor beyond anti-proliferation, that is, anti-inflammatory activities, implicate that it may be applicable to the treatment of atherosclerotic vascular diseases as well as post-intervention restenosis.

In the resent study, we did not investigate the mechanism by which nutlin-3 suppressed VSMC migration. Nutlin-3 inhibits cancer cell migration via cytoskeletal rearrangement in a p53-dependent manner.[38] Reportedly, p53 inhibits cell migration by regulation of Cdc42 and Rac1 pathways.[39, 40] While we speculate that nutlin-3 inhibits VSMC migration through p53-mediated suppression of Rho GTPases, further examination is required.

The limitation of the present study is that we did not verify the effects of nutlin-3 on neointima formation in p53-deficient mice to establish the definite link between the effects of nutlin-3 and p53 in vivo. However, we observed that nutlin-3 failed to inhibit cell cycle progression and NF-kB activation in p53-knocked down VSMCs and p53-deficient VSMCs, strongly suggesting that the effects of nutlin-3 depend on p53. Furthermore, there are many reports demonstrating that in vivo administration of nutlin-3 suppressed the growth of tumors with wild-type p53 whereas treatment with nutlin-3 did not affect the growth of p53-deficient or mutant

p53-bearing tumors in mice.[17, 18, 41] These findings including our results suggest that the pharmacological action of nutlin-3 in vivo is dependent on p53 as well. For another point, we cannot exclude possible secondary effects of nutlin-3 on neointima formation by way of, for example, inhibition of systemic cytokine expression and direct inhibitory effects on inflammatory cells such as macrophages and leukocytes. Further investigations are required on this point.

In conclusion, p53 activation by MDM2 inhibition prevented cellular proliferation, migration, and NF-κB activation in VSMCs; and besides attenuated neointimal hyperplasia with prevention of vascular proliferation and inflammatory responses. Targeting MDM2-p53 interaction might be a novel therapeutic strategy for treatment of vascular proliferative diseases.

Acknowledgements

We thank the Research Support Center, Kyushu University Graduate School of Medical Sciences for technical supports.

Funding

This work was supported in part by Grants-in-Aid for Scientific Research from the Ministry of Education, Culture, Sports, Science, and Technology of Japan (19590867).

Conflict of Interests

None declared.

References

1. Libby P. Inflammation in atherosclerosis. *Nature.* 2002;**420**:868-874.

2. Dzau VJ, Braun-Dullaeus RC, Sedding DG. Vascular proliferation and atherosclerosis: new perspectives and therapeutic strategies. *Nat Med.* 2002;**8**:1249-1256.

3. Costa MA, Simon DI. Molecular basis of restenosis and drug-eluting stents. *Circulation.* 2005;**111**:2257-2273.

4. Riley T, Sontag E, Chen P, Levine A. Transcriptional control of human p53-regulated genes. *Nat Rev Mol Cell Biol.* 2008;**9**:402-412.

5. Guevara NV, Kim HS, Antonova EI, Chan L. The absence of p53 accelerates atherosclerosis by increasing cell proliferation in vivo. *Nat Med.* 1999;**5**:335-339.

6. van Vlijmen BJ, Gerritsen G, Franken AL, Boesten LS, Kockx MM, Gijbels MJ *et al.* Macrophage p53 deficiency leads to enhanced atherosclerosis in APOE*3-Leiden transgenic mice. *Circ Res.* 2001;**88**:780-786.

7. Merched AJ, Williams E, Chan L. Macrophage-specific p53 expression plays a crucial role in atherosclerosis development and plaque remodeling. *Arterioscler Thromb Vasc Biol.* 2003;**23**:1608-1614.

8. Mercer J, Figg N, Stoneman V, Braganza D, Bennett MR. Endogenous p53 protects vascular smooth muscle cells from apoptosis and reduces atherosclerosis in ApoE knockout mice. *Circ Res.* 2005;**96**:667-674.

9. von der Thusen JH, van Vlijmen BJ, Hoeben RC, Kockx MM, Havekes LM, van Berkel TJ *et al.* Induction of atherosclerotic plaque rupture in apolipoprotein E-/- mice after adenovirus-mediated transfer of p53. *Circulation.* 2002;**105**:2064-2070.

10. Toledo F, Wahl GM. MDM2 and MDM4: p53 regulators as targets in anticancer therapy. *Int J Biochem Cell Biol.* 2007;**39**:1476-1482.

11. Toledo F, Wahl GM. Regulating the p53 pathway: in vitro hypotheses, in vivo veritas. *Nat Rev Cancer.* 2006;**6**:909-923.

12. Ihling C, Haendeler J, Menzel G, Hess RD, Fraedrich G, Schaefer HE *et al.* Co-expression of p53 and MDM2 in human atherosclerosis: implications for the regulation of cellularity of atherosclerotic lesions. *J Pathol.* 1998;**185**:303-312.

13. Nakamura Y, Suzuki S, Suzuki T, Ono K, Miura I, Satoh F *et al.* MDM2: a novel mineralocorticoid-responsive gene involved in aldosterone-induced human vascular structural remodeling. *Am J Pathol.* 2006;**169**:362-371.

14. Vassilev LT, Vu BT, Graves B, Carvajal D, Podlaski F, Filipovic Z *et al.* In vivo

activation of the p53 pathway by small-molecule antagonists of MDM2. *Science.* 2004;**303**:844-848.

15. Vassilev LT. MDM2 inhibitors for cancer therapy. *Trends Mol Med.* 2007;**13**:23-31.

16. Sarek G, Kurki S, Enback J, Iotzova G, Haas J, Laakkonen P *et al.* Reactivation of the p53 pathway as a treatment modality for KSHV-induced lymphomas. *J Clin Invest.* 2007;**117**:1019-1028.

17. Van Maerken T, Ferdinande L, Taildeman J, Lambertz I, Yigit N, Vercruysse L *et al.* Antitumor activity of the selective MDM2 antagonist nutlin-3 against chemoresistant neuroblastoma with wild-type p53. *J Natl Cancer Inst.* 2009;**101**:1562-1574.

18. Tovar C, Rosinski J, Filipovic Z, Higgins B, Kolinsky K, Hilton H *et al.* Small-molecule MDM2 antagonists reveal aberrant p53 signaling in cancer: implications for therapy. *Proc Natl Acad Sci U S A.* 2006;**103**:1888-1893.

19. Endo S, Yamato K, Hirai S, Moriwaki T, Fukuda K, Suzuki H *et al.* Potent in vitro and in vivo antitumor effects of MDM2 inhibitor nutlin-3 in gastric cancer cells. *Cancer Sci.* 2011;**102**:605-613.

20. Sata M, Maejima Y, Adachi F, Fukino K, Saiura A, Sugiura S *et al.* A mouse model of vascular injury that induces rapid onset of medial cell apoptosis

followed by reproducible neointimal hyperplasia. *J Mol Cell Cardiol.* 2000;**32**:2097-2104.

21. Andrae J, Gallini R, Betsholtz C. Role of platelet-derived growth factors in physiology and medicine. *Genes Dev.* 2008;**22**:1276-1312.

22. de Winther MP, Kanters E, Kraal G, Hofker MH. Nuclear factor kappaB signaling in atherogenesis. *Arterioscler Thromb Vasc Biol.* 2005;**25**:904-914.

23. Liu G, Park YJ, Tsuruta Y, Lorne E, Abraham E. p53 Attenuates lipopolysaccharide-induced NF-kappaB activation and acute lung injury. *J Immunol.* 2009;**182**:5063-5071.

24. Dey A, Wong ET, Bist P, Tergaonkar V, Lane DP. Nutlin-3 inhibits the NFkappaB pathway in a p53-dependent manner: implications in lung cancer therapy. *Cell Cycle.* 2007;**6**:2178-2185.

25. Secchiero P, Corallini F, Rimondi E, Chiaruttini C, di Iasio MG, Rustighi A *et al.* Activation of the p53 pathway down-regulates the osteoprotegerin expression and release by vascular endothelial cells. *Blood.* 2008;**111**:1287-1294.

26. Wadgaonkar R, Phelps KM, Haque Z, Williams AJ, Silverman ES, Collins T. CREB-binding protein is a nuclear integrator of nuclear factor-kappaB and p53 signaling. *J Biol Chem.* 1999;**274**:1879-1882.

27. Webster GA, Perkins ND. Transcriptional cross talk between NF-kappaB and

p53. *Mol Cell Biol.* 1999;**19**:3485-3495.

28. Yonemitsu Y, Kaneda Y, Tanaka S, Nakashima Y, Komori K, Sugimachi K *et al.* Transfer of wild-type p53 gene effectively inhibits vascular smooth muscle cell proliferation in vitro and in vivo. *Circ Res.* 1998;**82**:147-156.

29. Matsushita H, Morishita R, Aoki M, Tomita N, Taniyama Y, Nakagami H *et al.* Transfection of antisense p53 tumor suppressor gene oligodeoxynucleotides into rat carotid artery results in abnormal growth of vascular smooth muscle cells. *Circulation.* 2000;**101**:1447-1452.

30. George SJ, Angelini GD, Capogrossi MC, Baker AH. Wild-type p53 gene transfer inhibits neointima formation in human saphenous vein by modulation of smooth muscle cell migration and induction of apoptosis. *Gene Ther.* 2001;**8**:668-676.

31. Mayr U, Mayr M, Li C, Wernig F, Dietrich H, Hu Y *et al.* Loss of p53 accelerates neointimal lesions of vein bypass grafts in mice. *Circ Res.* 2002;**90**:197-204.

32. Sata M, Tanaka K, Ishizaka N, Hirata Y, Nagai R. Absence of p53 leads to accelerated neointimal hyperplasia after vascular injury. *Arterioscler Thromb Vasc Biol.* 2003;**23**:1548-1552.

33. Wan S, George SJ, Nicklin SA, Yim AP, Baker AH. Overexpression of p53 increases lumen size and blocks neointima formation in porcine interposition

vein grafts. *Mol Ther.* 2004;**9**:689-698.

34. Sanz-Gonzalez SM, Barquin L, Garcia-Cao I, Roque M, Gonzalez JM, Fuster JJ *et al.* Increased p53 gene dosage reduces neointimal thickening induced by mechanical injury but has no effect on native atherosclerosis. *Cardiovasc Res.* 2007;**75**:803-812.

35. Aylon Y, Oren M. Living with p53, dying of p53. *Cell.* 2007;**130**:597-600.

36. Secchiero P, Corallini F, Gonelli A, Dell'Eva R, Vitale M, Capitani S *et al.* Antiangiogenic activity of the MDM2 antagonist nutlin-3. *Circ Res.* 2007;**100**:61-69.

37. Perlman H, Maillard L, Krasinski K, Walsh K. Evidence for the rapid onset of apoptosis in medial smooth muscle cells after balloon injury. *Circulation.* 1997;**95**:981-987.

38. Moran DM, Maki CG. Nutlin-3a induces cytoskeletal rearrangement and inhibits the migration and invasion capacity of p53 wild-type cancer cells. *Mol Cancer Ther*;**9**:895-905.

39. Gadea G, Lapasset L, Gauthier-Rouviere C, Roux P. Regulation of Cdc42-mediated morphological effects: a novel function for p53. *Embo J.* 2002;**21**:2373-2382.

40. Guo F, Gao Y, Wang L, Zheng Y. p19Arf-p53 tumor suppressor pathway

regulates cell motility by suppression of phosphoinositide 3-kinase and Rac1 GTPase activities. *J Biol Chem.* 2003;**278**:14414-14419.

41. Sur S, Pagliarini R, Bunz F, Rago C, Diaz LA, Jr., Kinzler KW *et al.* A panel of isogenic human cancer cells suggests a therapeutic approach for cancers with inactivated p53. *Proc Natl Acad Sci U S A.* 2009;**106**:3964-3969.

Figure Lgends

Figure 1. Effects of nutlin-3 on proliferation, migration, and p53 pathways in VSMCs. (A) VSMCs pretreated with nutlin-3 for 6 hours were stimulated with PDGF-BB (50 ng/mL) for 24 hours and [^{3}H]-thymidine incorporation was counted. *****p<0.05, **p<0.01 vs PDGF(-)-Nutlin-3(-); † p<0.05, † † p<0.01 vs PDGF(+)-Nutlin-3(-) (n=3). **(B)** Effects of nutlin-3 on VSMC migration by *in vitro* scratch assay. VSMC monolayers were scratched and then stimulated with PDGF-BB (50 ng/mL) for 24 hours in the presence or absence of nutlin-3. Nuclei were stained with DAPI. Representative microphotographs and the quantitative analysis are shown. *p<0.005 vs control, † p<0.05 vs PDGF (n=3). **(C)** The expression levels of p53, p21, and MDM2 in VSMCs stimulated with nutlin-3 (10 μmol/L) were assessed by Western blot analysis. Histone H3 was used for loading control. The same results were obtained in three other independent experiments. **(D)** The effect of nutlin-3 on VSMC apoptosis was analyzed by flow cytometry. After pretreatment with nutlin-3 (10 μmol/L) for 24 hours and incubation with H_2O_2 (5 mmol/L) for 1 hour, VSMCs were stained with PI and Annexin V-FITC. The percentage of apoptotic cells (Annexin V-positive and PI-negative fraction) is shown. n.s.: not significant (n=3). Values represent mean±SEM.

Figure 2. Nutlin-3 induces cell cycle arrest in a p53-dependent manner in VSMC.

(A) The expression levels of p53 mRNA in VSMCs transfected with p53-targeting siRNA (25 nmol/L) or negative control siRNA (25 nmol/L) for 48 hours were assessed by RT-qPCR (n=4). NT: non-treated. n.s.: not significant. **(B)** Cell cycle profile analyzed by flow cytometry. VSMCs transfected with p53-siRNA (25 nmol/L) or control siRNA (25 nmol/L) were pretreated with nutlin-3 (10 μmol/L) for 6 hours and then stimulated with PDGF-BB (50 ng/mL) for 24 hours. Representative histograms and the percentage of cell cycle distribution are shown. CTRL: control, NUT: nutlin-3. *p<0.05 vs control, †p<0.01 vs PDGF (n=3 each).

Figure 3. Nutlin-3 attenuates neointimal hyperplasia after vascular injury. (A) Femoral arteries at 28 days after vascular injury (elastica van Gieson staining). Arrows indicate external elastic lamina. Arrowheads indicate internal elastic lamina. **(B)** Intimal area, medial area, intima/media (I/M) area ratio, and percent stenosis at 28 days after injury were analyzed. Values represent mean±SEM. *p<0.05 vs control, **p<0.01 vs control (control n=9, nutlin-3 n=7). **(C)** Wire-injured arteries (28 days) stained with FITC-conjugated anti-α-SMA antibody. Green: α-SMA. Blue: nuclei (DAPI). **(D)** Sirius red staining of injured vessels (28 days). Collagen fibers were stained in red

(upper panels). The Sirius Red-stained tissue specimens identical to upper panels were observed by polarizing microscopy (lower panels). **(E)** Immunostaining of PECAM-1 in vascular tissues at 28 days after injury. **(F)** Immunostaining of p53, p21, and MDM2 in the injured vessels (28 days). The same results were obtained in other samples (control n=9, nutlin-3 n=7).

Figure 4. Modulation of vascular proliferation and inflammatory responses by MDM2 inhibition. (A) Cell proliferation was assessed by BrdU incorporation at 14 days and 28 days after vascular injury. (Upper) Representative micrographs are shown. Arrowheads indicate internal elastic lamina. (Lower) Quantitative analysis of BrdU-positive cells in the neointima and the media. *$p<0.05$. n.s.: not significant. (14 d: control n=15, nutlin-3 n=11. 28 d: control n=9, nutlin-3 n=7). **(B)** (Upper) Apoptotic cells assessed by TUNEL method at 7, 14, and 28 days after injury. Arrows indicate TUNEL-positive cells. Positive control was the tissue specimen biochemically treated with DNase I, while negative control was the specimen incubated without TdT. (Lower) Quantitative analysis of TUNEL-positive cells in the neointima and media at 7 days after injury. n.s.: not significant. (control: n=7, nutlin-3: n=8). **(C)** Infiltration of inflammatory cells at 7days after vascular injury. Macrophages were immunostained with anti-Mac-3 antibody. T lymphocytes were stained with anti-CD3 antibody. **(D)**

Quantitative analysis of the number of inflammatory cells which infiltrated per section. *p<0.05 vs control (n=5 each).

Figure 5. Effects of MDM2 inhibition on inflammatory gene expression and NF-κB transcriptional activity. (A) mRNA expression levels of CCL5, IL-6, and ICAM-1 at 7 days after vascular injury were determined by RT-qPCR. C: control, N: nutlin-3. *p<0.005 vs control (uninjured); †p<0.05, ††p<0.01 vs control (injured) (control n=10, nutlin-3 n=10). Values represent mean±SEM. **(B)** Effect of nutlin-3 on NF-κB transactivation in VSMCs was assessed by DNA-binding ELISA for NF-κB p65. VSMCs transfected with control siRNA or p53-siRNA were stimulated with TNFα (20 ng/mL) for 1 hour after pretreatment with nutlin-3 (10 μmol/L) for 24 hours (n=3 each). Values represent mean ± SEM. CTRL: control, NUT: nutlin-3. *p<0.05, **p<0.001 vs control, †p<0.05 vs TNFα, n.s.: not significant (n=3).

Figure 1

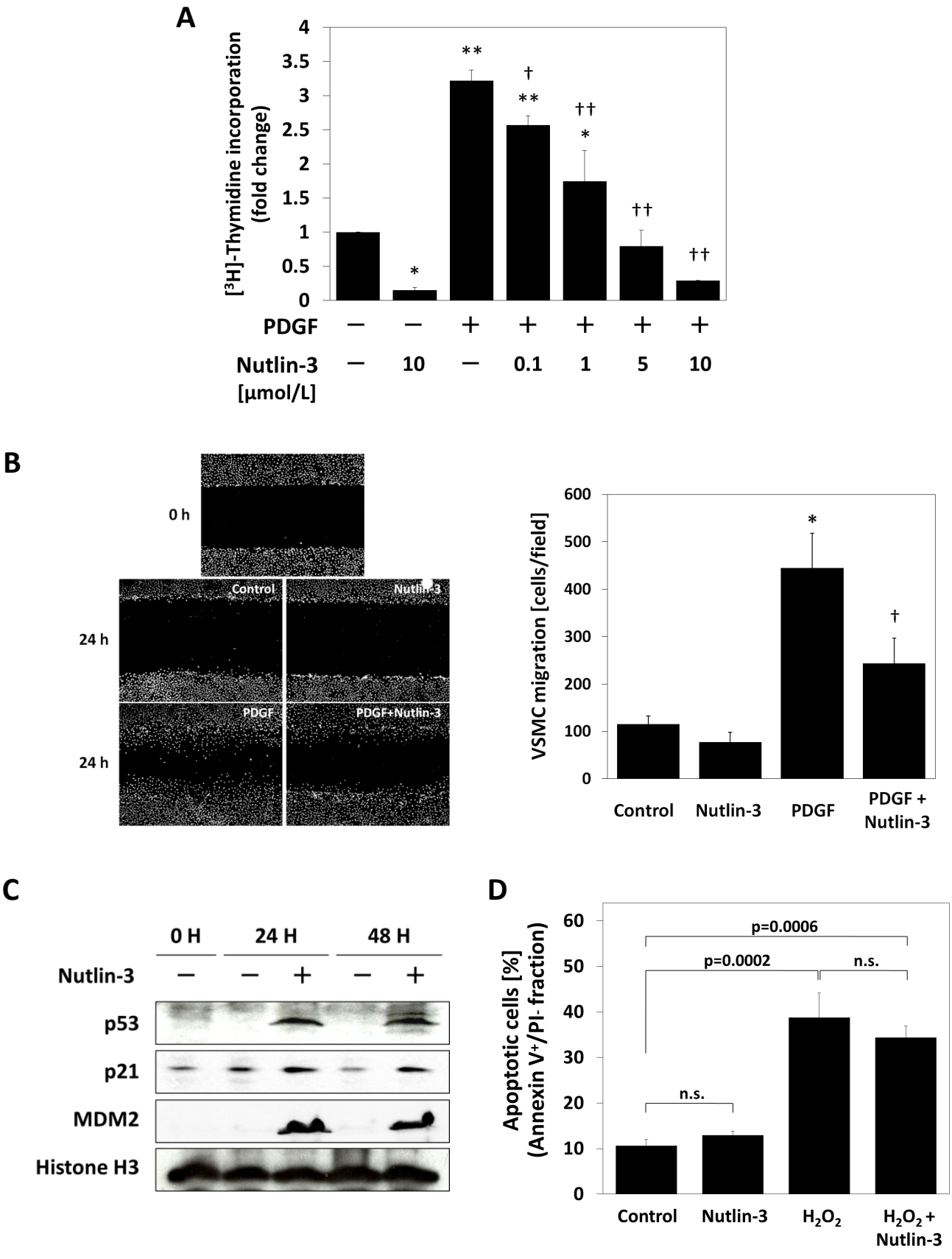
A
[³H]-Thymidine incorporation (fold change)
PDGF
Nutlin-3 [µmol/L]
B
0 h
24 h
Control
Nutlin-3
PDGF
PDGF+Nutlin-3
VSMC migration [cells/field]
Control
Nutlin-3
PDGF
PDGF + Nutlin-3
C
0 H
24 H
48 H
Nutlin-3
p53
p21
MDM2
Histone H3
D
Apoptotic cells [%] (Annexin V+/PI- fraction)
p=0.0006
p=0.0002
n.s.
n.s.
Control
Nutlin-3
H2O2
H2O2 + Nutlin-3

Figure 2

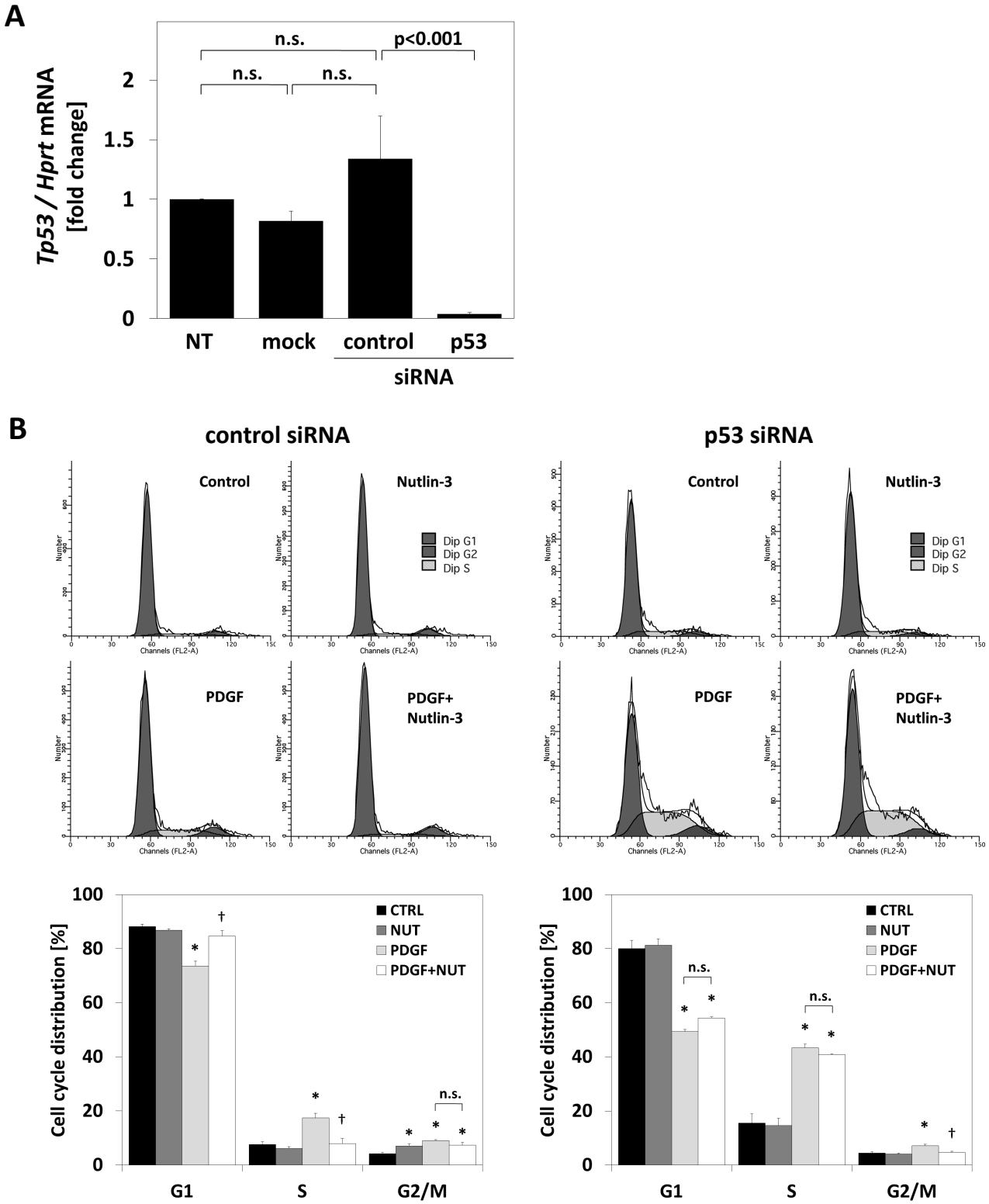
A
n.s.
p<0.001
n.s.
n.s.
Tp53 / Hprt mRNA [fold change]
2
1.5
1
0.5
0
NT
mock
control
p53
siRNA
B
control siRNA
p53 siRNA
Control
Nutlin-3
PDGF
PDGF+ Nutlin-3
Dip G1
Dip G2
Dip S
Number
Channels (FL2-A)
CTRL
NUT
PDGF
PDGF+NUT
Cell cycle distribution [%]
G1
S
G2/M
n.s.

Figure 3

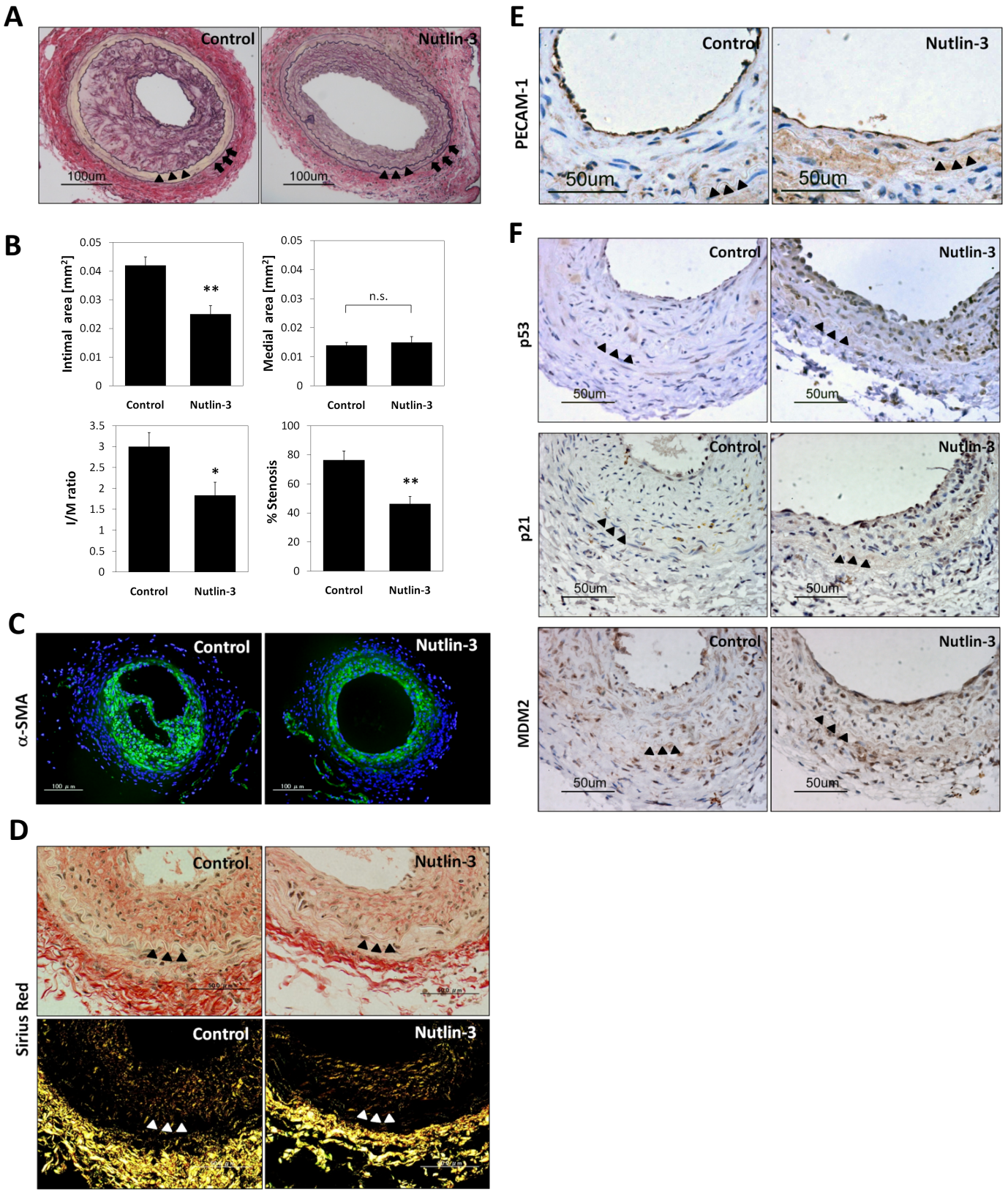
A
Control
Nutlin-3
100um
100um
B
Intimal area [mm²]
0.05
0.04
0.03
0.02
0.01
0
**
Control
Nutlin-3
Medial area [mm²]
n.s.
I/M ratio
3.5
3
2.5
2
1.5
1
0.5
*
% Stenosis
100
80
60
40
20
**
C
α-SMA
D
Sirius Red
E
PECAM-1
50um
F
p53
p21
MDM2

Figure 4

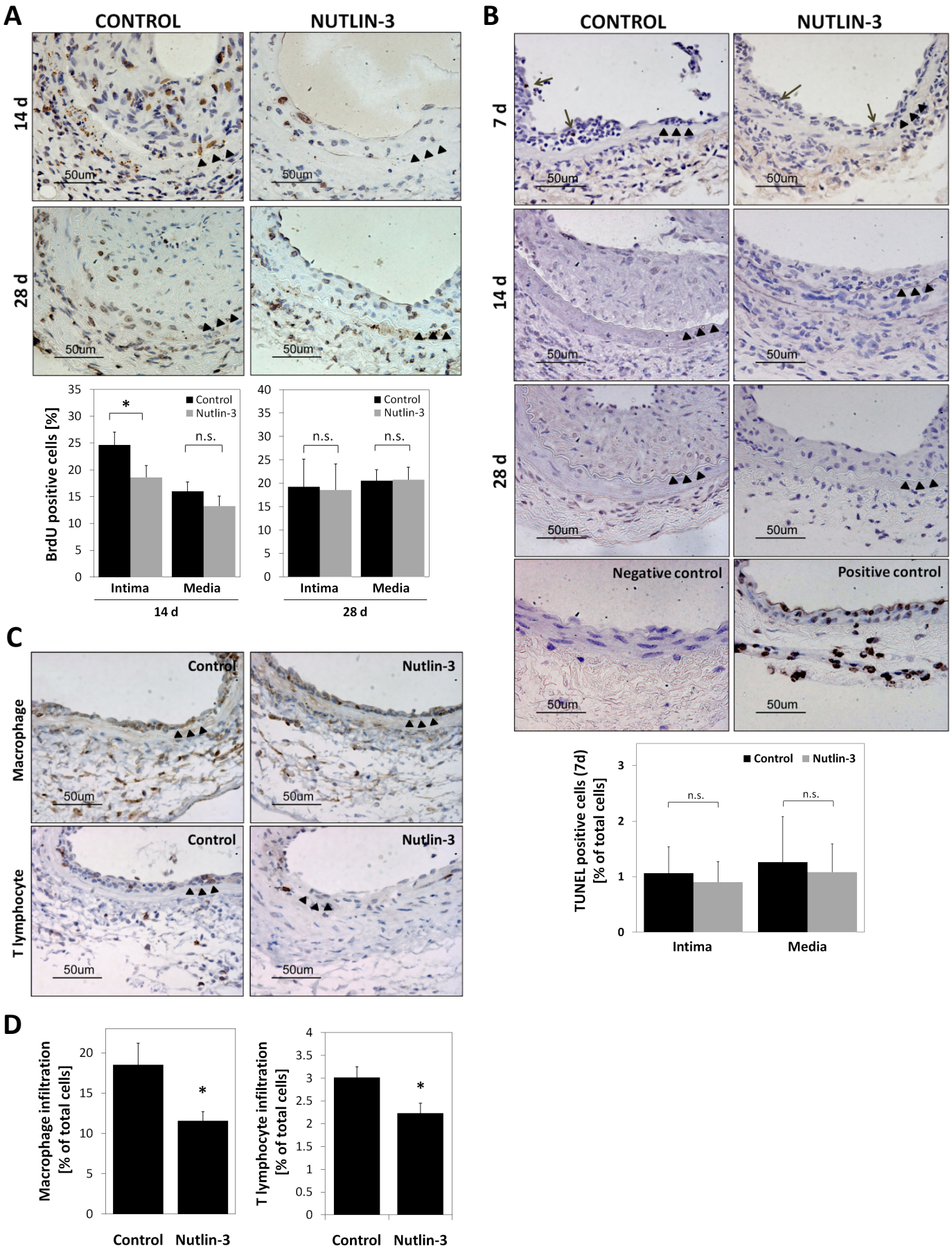
A
CONTROL
NUTLIN-3
14 d
28 d
50um
BrdU positive cells [%]
Control
Nutlin-3
*
n.s.
Intima
Media
14 d
28 d
B
CONTROL
NUTLIN-3
7 d
14 d
28 d
Negative control
Positive control
TUNEL positive cells (7d) [% of total cells]
C
Macrophage
T lymphocyte
Control
Nutlin-3
D
Macrophage infiltration [% of total cells]
T lymphocyte infiltration [% of total cells]
Control
Nutlin-3

Figure 5

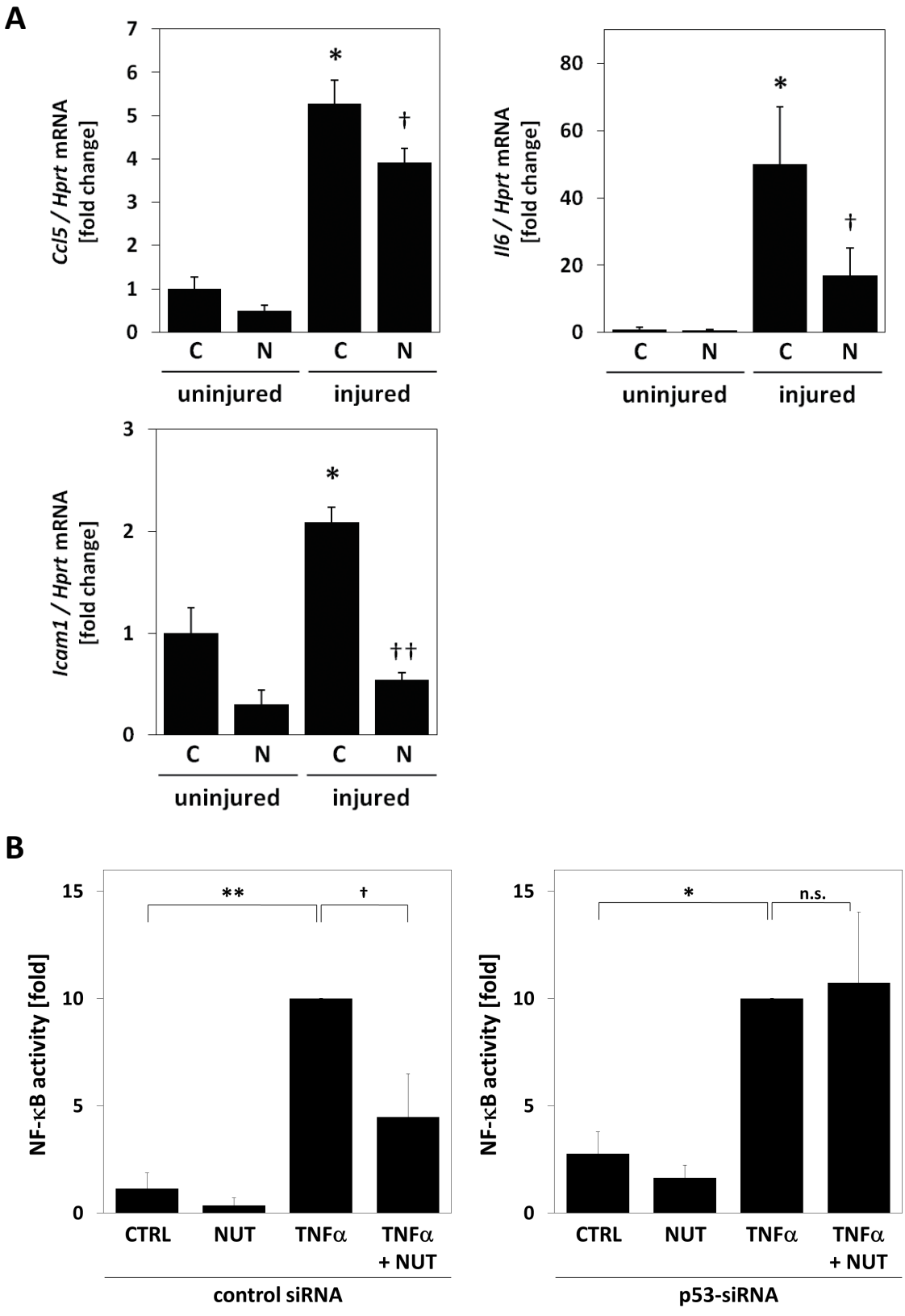
A
Ccl5 / Hprt mRNA [fold change]
7
6
5
4
3
2
1
0
*
†
C
N
C
N
uninjured
injured
Il6 / Hprt mRNA [fold change]
80
60
40
20
0
*
†
C
N
C
N
uninjured
injured
Icam1 / Hprt mRNA [fold change]
3
2
1
0
*
††
C
N
C
N
uninjured
injured
B
NF-κB activity [fold]
15
10
5
0
**
†
CTRL
NUT
TNFα
TNFα + NUT
control siRNA
NF-κB activity [fold]
15
10
5
0
*
n.s.
CTRL
NUT
TNFα
TNFα + NUT
p53-siRNA